Original Article

DOI: 10.5582/ddt.2025.01121

Development of ginger extract-loaded self-nanoemulsifying drug delivery system for enhanced solubility of ginger extract

Maung Maung Than[1], Chuda Chittasupho[2], Songwut Yotsawimonwat[2], Kantaporn Kheawfu[2,*]

[1] Ph.D. Degree Program in Pharmacy, Faculty of Pharmacy, Chiang Mai University, Chiang Mai, Thailand;
[2] Department of Pharmaceutical Sciences, Faculty of Pharmacy, Chiang Mai University, Chiang Mai, Thailand.

SUMMARY: The well-known medicinal plant ginger (*Zingiber officinale* Roscoe) has numerous health benefits, but its key bioactive compound, 6-gingerol, suffers from poor water solubility and stability. This study aimed to enhance the oral delivery of ginger extract by formulating a self-nanoemulsifying drug delivery system (SNEDDS) using a design of experiments (DoE) approach. Ginger rhizomes were extracted by ultrasound-assisted extraction, with a 10-min extraction time yielding the highest 6-gingerol content. An I-optimal mixture design was then applied to develop SNEDDS formulations using castor oil, Cremophor RH40, various co-surfactants (Span 20 or Span 80), and co-solvents (polyethyleneglycol 400 (PEG 400) or ethanol). The optimized SNEDDS readily self-emulsified in gastric medium, producing nano-sized droplets (42.5-78.1 nm) with low polydispersity (0.12-0.58) within 10 min. The ginger extract-loaded SNEDDS (G-SNEDDS) achieved high encapsulation efficiencies, exceeding 90% for both 6-gingerol and 6-shogaol, and significantly enhanced the *in vitro* release of 6-gingerol, reaching cumulative release levels of approximately 90-100% over 48 h, compared to only 67% from the unformulated extract. Transmission electron microscopy (TEM) confirmed the formation of uniform, spherical nanoemulsion droplets. Short-term stability testing indicated that the optimized formulation remained physically stable, as evidenced by minimal changes in droplet size, and preserved most of the 6-gingerol content under ambient storage conditions; however, exposure to elevated temperatures accelerated the conversion of 6-gingerol to 6-shogaol. Overall, the optimized SNEDDS significantly enhanced the solubility, dissolution, and storage stability of ginger extract, offering a promising strategy to improve the oral bioavailability of the therapeutically active constituents present in ginger.

Keywords: ginger extract, self-nanoemulsifying drug delivery systems (SNEDDS), lipid-based formulation, 6-gingerol, 6-shogaol

1. Introduction

The well-known medicinal plant ginger (*Zingiber officinale* Roscoe) has been traditionally used for centuries to treat a variety of ailments. It possesses a wide range of pharmacological properties, including anti-inflammatory, antioxidant, anti-nausea, antimicrobial, anticancer, anti-ulcer, antidiabetic, and immunomodulatory effects, mainly attributed to its bioactive constituents such as gingerols and shogaols (*1-3*). Despite these promising biological activities, the use of ginger extract as an antioxidant is often limited due to the chemical instability of its active constituents. These compounds are volatile and sensitive to environmental factors such as light, air, and heat, which negatively affect their solubility, stability, and ultimately, their bioavailability (*4*).

Among the major active components, 6-gingerol is the most abundant and extensively studied. However, it exhibits poor aqueous solubility, contributing to its low oral bioavailability. It dissolves more readily in organic solvents such as ethanol (30 mg/mL), dimethylformamide (DMF, 30 mg/mL), and dimethyl sulfoxide (DMSO, 25 mg/mL), whereas its solubility in phosphate-buffered saline (PBS, pH 7.2) is significantly lower, approximately 1 mg/mL (*5,6*). This limited aqueous solubility presents a major challenge for formulating effective oral dosage forms. Despite these limitations, plant-derived medications, including ginger-based preparations, are generally more accessible and cost-effective and are associated with fewer adverse effects than synthetic drugs (*7*).

To overcome the challenges associated with the poor solubility and instability of ginger extract, various advanced drug delivery systems have been investigated. Nanostructured lipid carriers have been reported to enhance the aqueous solubility of 6-gingerol and improve its antioxidant and anti-inflammatory activities

(*8*). Chitosan-based nanoparticles containing gingerol demonstrated improved anticancer efficacy by markedly increasing cancer cell inhibition within 48 h (*9*). In addition, microemulsion-based delivery systems have been shown to improve the solubility, stability, and anti-inflammatory effects of ginger extract (*10*).

One promising strategy is the self-nanoemulsifying drug delivery system (SNEDDS), which consists of an isotropic mixture of oil, surfactant, and co-surfactant. SNEDDS can spontaneously form fine oil-in-water nanoemulsions (< 200 nm) upon contact with aqueous media in the gastrointestinal tract, thereby improving solubilization, absorption, and stability of lipophilic drugs. A self-microemulsifying drug delivery system (SMEDDS) containing 6-gingerol reported enhanced release in various pH media and prolonged systemic exposure (6.58-fold) compared to the unformulated extract (*11*). Similarly, SNEDDS containing ginger extract using snakehead fish oil have demonstrated improved *in vivo* antioxidant activity, as evidenced by increased superoxide dismutase levels, despite slightly lower *in vitro* radical-scavenging activity (*12*). These findings collectively highlight the potential of SNEDDS in addressing the challenges associated with ginger extract delivery. Nonetheless, further optimization and evaluation of the formulation are necessary to ensure efficacy and safety.

Design of experiment (DoE) is a powerful statistical tool used in pharmaceutical development to optimize formulation parameters and identify critical variables affecting product performance (*13*). In the context of SNEDDS development, formulation factors such as the type and concentration of oil, surfactant, and co-surfactant can be systematically varied to study their impact on droplet size, polydispersity index (PDI), and other critical quality attributes (*14*). This approach is more efficient than traditional trial-and-error methods, reducing time and resources required for formulation development.

Therefore, the objective of this study was to develop a ginger extract-loaded SNEDDS (G-SNEDDS) using a DoE-based approach and to evaluate the physicochemical properties of the resulting formulation.

2. Materials and Methods

2.1. Materials

Standard 6-gingerol (6G) was purchased from Sigma-Aldrich (Burlington, MA, USA) Acetonitrile and methanol (high-performance liquid chromatography (HPLC) grade) as well as ethanol (AR grade), were purchased from RCI Labscan (Bangkok, Thailand). Ultrapure water used throughout this study was obtained from a Milli-Q reverse osmosis (RO) system, Maxima (Merck Millipore, Burlington, MA, USA). Castor oil, Cremophor RH 40 (polyethylene glycol-40 hydrogenated castor oil), Tween 80 (polyoxyethylene sorbitan mono oleate), Span 80 (sorbitan mono oleate), and Span 20 (sorbitan mono laurate) were purchased from Namsiang Company Limited (Bangkok, Thailand). Polyethyleneglycol 400 (PEG 400) was purchased from Srichand United Dispensary (Bangkok, Thailand).

2.2. Extraction method for ginger rhizomes

The 1-year-old ginger rhizomes were sourced from Samoeng District in Chiang Mai Province, and obtained from a local market in Chiang Mai, Thailand. The extraction method was adapted from a previously published method (*15*). The rhizomes were preliminary cleaned to remove impurities and excess moisture, then peeled and sliced into thin pieces (approximately 3 mm thick). The sliced rhizomes were dried in a controlled oven at 50ºC for 24 h. The dried slices were subsequently ground into a fine powder (< 200 mesh) using an electric blade mill. The powdered ginger was stored at room temperature prior to extraction.

Ultrasound-assisted extraction (UAE) was performed using an ultrasonic bath. For each experiment, 0.3 g of ginger powder was mixed with 20 mL of 95% ethanol in centrifuge tubes. Extraction times of 10, 20, and 30 min were evaluated while maintaining the extraction temperature below 60ºC. After extraction, the mixtures were filtered through Whatman No. 1 filter paper. The filtrates were then concentrated to dryness using a rotary evaporator to determine the crude extract yield. The obtained extracts were stored in light-resistant containers at 4 ± 2ºC until further analysis. The percentage yield (% yield) was calculate using the following equation (1):

$$\% \text{ Yield} = \frac{\text{Crude Extract Weight}}{\text{Dried Sample Weight}} \times 100 \text{ -------- (1)}$$

2.3. Quantification of active compounds in ginger extract

The quantification of active constituents in ginger extract was performed using HPLC, with 6-gingerol and 6-shogaol as the reference standard. The analytical procedure was adapted from the Thai Herbal Pharmacopoeia 2021 (*16*). A stock solution of 6-gingerol and 6-shogaol was prepared with a concentration of 1 mg/mL. The stock solution was diluted to prepare a five-point calibration curve within the range of 0.0025-0.1 μg/mL. A quantity of 10 mg of dried ginger extract, or an appropriate amount, was accurately weighed and dissolved in methanol with gentle mixing.

The HPLC analysis was performed on an Agilent Technologies 1260 Series liquid chromatograph (Agilent Technologies, Pittsburgh, PA, USA) equipped with a quaternary pump, autosampler, thermostatic column chamber, and diode array detector (DAD). Detection was performed at 282 nm. Chromatographic separation was achieved on a C18 reverse-phase column (Knauer,

Berlin, Germany; Eurospher II 100-5, 250 × 4.6 mm, 5 µm). The mobile phase consisted of buffer solution (A) and acetonitrile (B), delivered at a flow rate of 1.0 mL/min. Mobile phase A was prepared by mixing 550 mL of acetonitrile, 440 mL of 0.1% phosphoric acid in water, and 10 mL of methanol. Gradient elution was applied as follows: 100% B at 0 min, decreasing to 0% B by 2 min and held until 12 min, then linearly increased to 100% B by 14 min and maintained until 35 min. Chromatographic analysis was performed in triplicate. The data were recorded and processed using Agilent Chemstation software (Agilent Technologies, Pittsburgh, PA, USA).

2.4. Development of the SNEDDS

2.4.1. Selection of oil, surfactant, co-surfactant, and co-solvent

A preliminary selection of excipients for the SNEDDS formulation was carried out based on a literature review. The chosen components included castor oil as the oil phase; Cremophor RH40 as the surfactants; Span 80 and Span 20 as co-surfactant; and PEG 400 and ethanol as co-solvents, owing to their emulsifying capacity, compatibility, and oral safety profiles. The maximum permissible oral dosage ranges of these components were also reviewed and considered in the experimental design.

2.4.2. Experimental design

The formulation optimization was performed using the Design-Expert® software (Version 13, Stat-Ease Inc., Minneapolis, MN, USA), employing an I-optimal mixture design. The design aimed to determine the optimal ratio of oil, surfactant, co-surfactant, and co-solvent for efficient self-nanoemulsification. Four formulation systems (Systems 1 to 4), each consisting of varying proportions of oil, surfactant, co-surfactant, and co-solvent, as detailed in Table 1, were studied. The independent variable ranges were set as follows: oil (5-40% w/w), surfactant combined with co-surfactant (50-85% w/w), and co-solvent (0-10% w/w). The composition of the 18 experimental formulations is shown in Table 2. Droplet size, size distribution, and self-emulsification time required to obtain uniform nanosized droplets of the dispersed SNEDDS were considered as response variables. The relationship between the response and the formulation variables was determined using a quadratic mixture model, as shown in Equation (2):

$$Y = m_1A + m_2B + m_3C + m_4D + m_5AB + m_6AC + m_7AD + m_8BC + m_9BD + m_{10}CD \quad (2)$$

where Y is the response variable, and m_1–m_{10} are the regression coefficients corresponding to the components A–D, which denote the proportions of oil, surfactant, co-surfactant, and co-solvent, respectively. The intercept term was omitted, as the model was fitted using mixture design coding, where the sum of all component proportions equals 100%. Model performance was evaluated using the coefficient of determination (R^2), adjusted R^2, and predicted R^2 values. R^2 and adjusted R^2 values close to 1 indicate a strong model fit, whereas a predicted R^2 value greater than 0.5 suggests good predictive ability.

2.4.3. Formulation preparation

Each formulation was prepared according to the composition specified in the design matrix. The respective quantities of oil, surfactant, co-surfactant, and co-solvent were accurately weighed and mixed thoroughly to obtain a homogenous preconcentrate suitable for self-nanoemulsification.

2.4.4. Evaluation of physical characteristics

The physical properties of the SNEDDS formulations were evaluated based on self-emulsification time, droplet size, and PDI. To assess emulsification performance, 1 mL of each formulation was added to 250 mL of 0.1 N hydrochloric acid maintained at 37 ± 0.5°C under gentle stirring. The time required for the formation of a clear or slightly bluish nanoemulsion was recorded. Droplet size and PDI were determined using dynamic light scattering (DLS) with a Zetasizer

Table 1. Type and composition ranges (% w/w) of components used in each SNEDDS system for experimental design

Component	System 1	System 2	System 3	System 4
Oil:				
Castor oil	5-40	5-40	5-40	5-40
Surfactant:				
Cremophor RH 40	0-85	0-85	0-85	0-85
Co-surfactant:				
Span 20	0-85	-	0-85	-
Span 80	-	0-85	-	0-85
Co-solvent:				
PEG 400	0-10	0-10	-	-
Ethanol	-	-	0-10	0-10

Table 2. Experimental compositions (% w/w) of SNEDDS formulations obtained from the I-optimal mixture design

Exp No. (System 1-4)	Composition (% w/w)			
	Oil (A)	Surfactant (B)	Co-surfactant (C)	Co-solvent (D)
1	40.0	60.0	0.0	0.0
2	40.0	26.7	24.9	8.4
3	40.0	9.7	40.3	10.0
4	37.3	0.0	61.2	1.5
5	32.8	44.9	12.2	10.0
6	23.8	39.2	31.9	5.2
7	23.8	39.2	31.9	5.2
8	23.8	39.2	31.9	5.2
9	22.6	0.0	67.4	10.0
10	22.1	17.3	50.6	10.0
11	20.8	69.2	0.0	10.0
12	15.0	35.6	49.4	0.0
13	15.0	35.6	49.4	0.0
14	11.7	85.0	0.0	3.3
15	10.2	0.0	85.0	4.8
16	5.6	63.0	21.4	10.0
17	5.0	16.2	68.8	10.0
18	5.0	44.0	41.0	10.0

Nano ZS (Malvern Instruments Ltd., Malvern, UK) after appropriate dilution (1:100, v/v) with distilled water to minimize multiple scattering effects.

2.4.5. Selection of the optimal SNEDDS formulation

The selection criteria included a self-emulsification time of ≤ 10 min, a mean droplet size ≤ 200 nm, and a PDI ≤ 0.3, indicating a narrow and uniform particle size distribution. Formulations that met all these parameters were considered suitable for oral delivery, as they demonstrated efficient spontaneous emulsification, nanoscale droplet formation, and consistent physical stability. These optimal formulations were subsequently selected for further investigation.

2.5. Preparation of G-SNEDDS

The ginger extract was initially dissolved in the selected co-solvent and subsequently combined with the surfactant and co-surfactant under continuous stirring. The oil phase was then gradually added to the mixture. The resulting system was vortexed overnight to ensure uniform dispersion and formation of a stable preconcentrate. The optimized G-SNEDDS formulation was stored in sealed amber glass vials at 4 ± 2°C until further analysis.

2.6. Determination of drug entrapment efficiency (EE)

The EE of 6-gingerol and 6-shogaol within the G-SNEDDS formulation was determined based on a method adapted from a previously published method (*17*). Briefly, ultrafiltration using a 3,500 Da molecular weight cut-off membrane was employed to separate free (unentrapped) 6-gingerol and 6-shogaol from the nanoemulsion. The samples were centrifuged at 10,000× *g* for 10 min, and the resulting filtrate was collected. The concentrations of 6-gingerol and 6-shogaol in the filtrate (free drug) and the SNEDDS (total drug) were quantified using HPLC. The entrapment efficiency was calculated using the following equation (3):

$$EE\ (\%) = (W_t - W_f)/W_t \times 100 \text{ ------- (3)}$$

where W_t is the total amount of 6-gingerol or 6-shogaol in the formulation and W_f is the amount of free (unentrapped) 6-gingerol or 6-shogaol in the filtrate.

2.7. Morphological characterization of G-SNEDDS

The morphology of the dispersed droplets was investigated using transmission electron microscopy (TEM), according to a previous report (*18*), with some modifications. In brief, the samples were prepared by diluting 1 g of G-SNEDDS with 100 mL of 0.1 N hydrochloric acid and gently mixing them using a magnetic stirrer at 100 rpm. Subsequently, the sample was placed on copper grids (200 mesh), then the dried sample was stained with 1% phosphotungstic acid and dried at 25°C overnight. After that, the grid was loaded into a TEM sample holder. The droplet morphology was observed and recorded using a JEM 2100 Plus TEM (JEOL Ltd., Tokyo, Japan) with an energy filter installed (Omega filter, JEOL Co., Tokyo, Japan) and was operated at 100 kV.

2.8. *In vitro* drug release study

The *in vitro* drug release profile of the G-SNEDDS was evaluated using the dialysis bag diffusion method. The release medium was 0.1 N hydrochloric acid. In each

experiment, 1 g of G-SNEDDS was diluted with an equal volume of the respective medium (1:1, w/v) and placed in a dialysis bag, which was then immersed in 100 mL of fresh release medium contained in a 150 mL beaker. The system was maintained at 37 ± 0.5°C in a thermostatic shaking water bath set at 100 rpm. Samples were collected at predetermined time intervals over a 48 h period. At each time point, a 10 mL aliquot of the release medium was withdrawn and immediately replaced with an equal volume of fresh medium to maintain sink conditions. Each formulation was tested in triplicate. The collected samples were analyzed using HPLC at a detection wavelength of 282 nm to quantify the amount of 6-gingerol released as the major component. The cumulative percentage of drug release was calculated and plotted as a function of time.

2.9. Stability study of G-SNEDDS

The stability of the G-SNEDDS formulations was assessed using both heating-cooling cycle testing and a short-term storage stability study under different temperature conditions. For the heating-cooling test, each cycle involved storing the formulations at 4°C for 48 h, followed by 45°C for an additional 48 h. This cycle was repeated five times to simulate thermal stress. For the short-term stability study, the formulations were stored at 4°C, 30°C, and 45°C for a period of 90 days. Samples were withdrawn and analyzed at day 0, 30, 60, and 90. After each time point, physical stability was evaluated by measuring particle size and PDI using a Zetasizer Nano ZS. Chemical stability was assessed by determining the concentration of the active constituents, 6-gingerol and 6-shogaol, using a validated HPLC method. Formulations that maintained stable particle size distribution and retained chemical content over time were considered physically and chemically stable and were selected for further evaluation in subsequent studies.

2.10. Statistical analysis

Statistical analysis was performed using *t*-test and one-way analysis of variance (ANOVA) to identify significant differences among experimental groups. All results were expressed as mean ± standard deviation (SD). A p-value < 0.05 was considered statistically significant unless otherwise stated.

3. Results

3.1. Optimization of ginger extraction process

The results of ginger extraction at various extraction times are presented in Table 3. The crude extract obtained from dried ginger rhizomes appeared as a dark brown liquid. Among the tested durations (10, 20, and 30 min), the 10-min extraction yielded the lowest extract yield, whereas the 30-min extraction resulted in the highest yield ($p < 0.05$). Despite the higher yields at longer extraction times, the 6-gingerol content was significantly higher in the 10-min extract ($p < 0.05$), compared to those obtained at 20 and 30 min. In contrast, the 6-shogaol content did not differ significantly among the three extraction times. These findings indicate that although prolonged extraction enhances overall yield, due to increased cell wall disruption and improved solvent penetration, shorter extraction durations better preserve thermolabile constituents, such as 6-gingerol. Therefore, the 10-min extraction condition was considered the most suitable for obtaining high levels of bioactive compounds, particularly 6-gingerol, under the tested conditions.

3.2. Preliminary screening and selection of SNEDDS systems

3.2.1. Effects of excipients on particle size

A comparative analysis was performed to evaluate four distinct SNEDDS platforms, each comprising castor oil as the lipid phase and Cremophor RH40 as the primary surfactant. The systems differed in their co-surfactant type (Span 20 or Span 80) and co-solvent (PEG 400 or ethanol) combinations. The formulations were assessed using an I-optimal mixture design fitted to a quadratic model to determine the effect of each excipient and their interactions on nanoemulsion performance. The studied response variables included droplet size, PDI, and self-emulsification time.

Among these outcomes, only droplet size demonstrated statistically acceptable model fitting, as evidenced by high R^2 and adjusted R^2 values and acceptable lack-of-fit results. Therefore, the regression coefficients and interaction effects are discussed primarily with respect to droplet size, which reflects

Table 3. Extract yield and contents of major bioactive compounds in ginger extracts obtained at different extraction times (mean ± SD, n = 3)

Extraction time	Yield (%)	6-Gingerol (mg/g crude extract)	6-Shogaol (mg/g crude extract)
10 min	10.17 ± 0.71^{a}	68.43 ± 5.00^{a}	6.55 ± 0.22^{c}
20 min	13.01 ± 0.03^{b}	43.34 ± 28.91^{b}	6.82 ± 0.14^{c}
30 min	14.67 ± 1.41^{c}	44.30 ± 19.04^{b}	7.39 ± 0.08^{c}

Different superscript letters indicate statistically significant differences among means ($p < 0.05$, one-way ANOVA with Tukey's post hoc test).

the efficiency of spontaneous nanoemulsion formation and is a critical parameter for drug solubilization and absorption.

Figure 1 presents the prediction contour plots of droplet size across Systems 1-4 at a fixed co-solvent concentration of 5% w/w, while Table 4 summarizes the regression coefficients and model parameters. System 4, composed of castor oil, Cremophor RH 40, Span 80, and ethanol, demonstrated superior statistical performance, with R^2 = 0.9865, adjusted R^2 = 0.9712, and predicted R^2 = 0.9455, indicating excellent model fit and predictive reliability. In contrast, System 3 (Span 20 and ethanol) showed the weakest model fit, suggesting that the formulation may be less consistent in behavior or less amenable to modeling within the chosen experimental range.

Among the individual terms, the co-solvent (D) exhibited the strongest influence on droplet size across all systems, particularly in System 1 (PEG 400-based), where the coefficient for co-solvent presented the highest value. This finding suggests a pronounced droplet size-increasing effect, likely attributable to the higher hydrophilicity and viscosity of PEG 400, which could interfere with efficient emulsification. On the other hand, System 4, which used ethanol as the co-solvent, exhibited a more moderate effect of co-solvent, indicating that ethanol facilitated improved emulsification and smaller droplet formation.

Several interaction terms were also significant. In System 1, the interactions AD, BD, and CD showed large negative coefficients, indicating negative effects between oil and co-solvent, and between other formulation components, in reducing droplet size. Although similar negative interaction trends were observed across all systems, these effects were less pronounced in ethanol-based systems. Notably, the AB interaction term (oil × surfactant) in System 4 was statistically significant ($p < 0.05$), demonstrating that the balance between oil and surfactant significantly impacted droplet size reduction in this ethanol-based formulation.

The beneficial role of Span 80, a low hydrophilic–lipophilic balance (HLB) surfactant, in Systems 2 and 4 may be attributed to its enhanced compatibility with castor oil, contributing to more efficient interfacial tension reduction and smaller droplet sizes. Overall, System 4 emerged as the most promising formulation, based on both statistical modeling outcomes and practical formulation considerations. The combination of Span 80 and ethanol provided the most favorable droplet size profile and robust model reliability, supporting its selection as a suitable candidate for further development

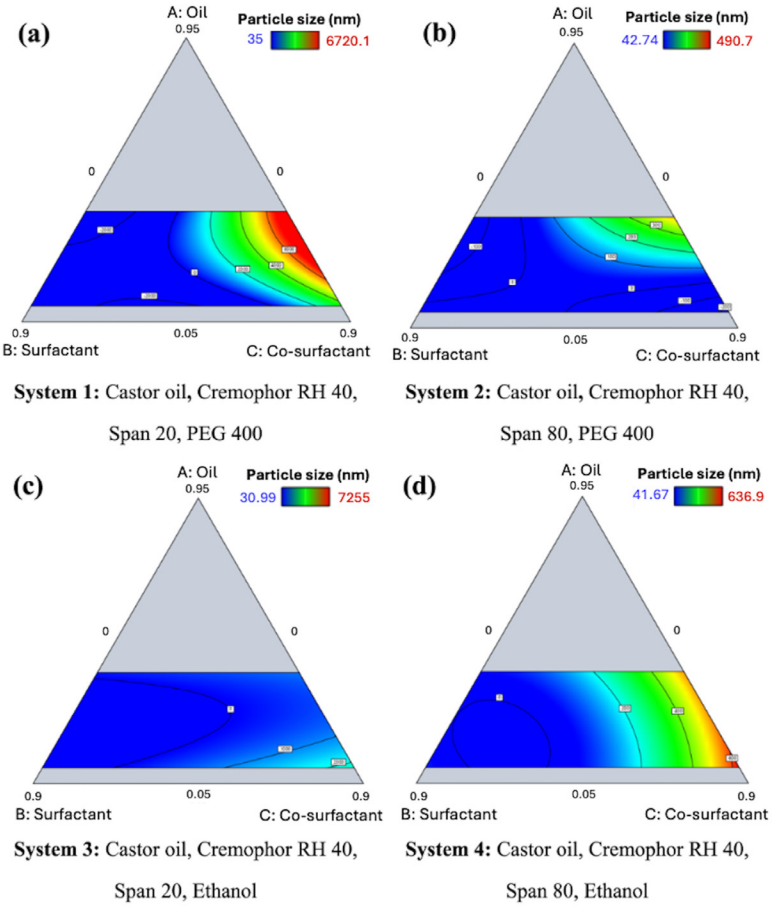

System 1: Castor oil, Cremophor RH 40, Span 20, PEG 400

System 2: Castor oil, Cremophor RH 40, Span 80, PEG 400

System 3: Castor oil, Cremophor RH 40, Span 20, Ethanol

System 4: Castor oil, Cremophor RH 40, Span 80, Ethanol

Figure 1. Prediction contour plots of droplet size (nm) after dispersing the SNEDDS system 1 (a), system 2 (b), system 3 (c), and system 4 (d) in 0.1 N hydrochloric acid. All systems were evaluated at a fixed co-solvent concentration of 5% w/w.

Table 4. Equation coefficients and model parameters for the fitted quadratic models for droplet size in each SNEDDS system

Parameters	System 1	System 2	System 3	System 4
A	-17755.29	1562.94	18600.97	1409.39
B	2595.31	315.65	1264.25	99.47
C	23.39	-333.42	1883.55	811.54
D	699700	62118.6	152200	11098.50
AB	21443.81	-2706.97	-29701.11	-2198.49*
AC	70696.81*	1263.12	-36392.36	-1495.01
AD	-821900*	-77500.6*	-171400	-15297.44
BC	-18728.71*	401.89	-359.86*	-1504.96*
BD	-790900*	-68930.5*	-187900	-11394.08
CD	-712600*	-66233.3*	-131900	-13495.91
R^2	0.984	0.952	0.548	0.986
R^2 adjusted	0.954	0.866	0.039	0.971
Predicted R^2	0.218	0.314	0.507	0.946

A, oil; B, surfactant; C, co-surfactant; D, co-solvent; the asterisks (*) signify coefficients relating to equation terms of significant effect on the response value.

and *in vivo* evaluation.

3.2.2. Effects of excipients on size distribution

The size distribution of the nanoemulsions, expressed as PDI, varied notably with the composition and relative proportions of excipients (Table 5). Formulations containing at least 35% w/w Cremophor RH40 and 20-35% w/w co-surfactant produced narrow size distributions (PDI = 0.12-0.20), as observed in Exp. 6-8 across Systems 2-4 and in Exp. 2 of all systems. In contrast, formulations with low surfactant content (≤ 10% w/w) and high co-surfactant levels (≥ 40% w/w), such as Exp. 3 and 10, exhibited high PDI values ranging from 0.84 to 1.00, indicating broad or multimodal particle size distributions. When comparing co-surfactants, Span 80 generally resulted in lower PDI values than Span 20, particularly in the presence of sufficient Cremophor RH40 (*e.g.*, System 2, Exp. 2 and 5-8). Ethanol-based systems (Systems 3 and 4) also achieved favorable PDI values (*e.g.*, System 4, Exp. 2: 0.17 and Exp. 18: 0.19).). However, increasing ethanol content combined with reduced Cremophor RH40 levels led to higher PDI values (*e.g.*, Exp. 3 and 10). In comparison, PEG 400–based systems (Systems 1 and 2) demonstrated a broader range of PDI values, ranging from 0.12 (System 2, Exp. 2) to 1.00 (System 1, Exp. 3, 10, and 17). Overall, formulations containing Span 80 and adequate levels of Cremophor RH40, in combination with either ethanol or moderate amounts of PEG 400, consistently produced the most uniform droplet size distributions (PDI ≤ 0.2).

3.2.3. Effects of excipients on self-emulsification time

The self-emulsification time of the four SNEDDS systems varied markedly depending on the type and proportion of excipients (Table 5). System 1, containing Span 20 and PEG 400, exhibited the fastest self-emulsification, with dispersion completed within approximately 1-3 min. In contrast, Systems 2-4 generally required longer emulsification times (> 10 min), except for formulations with higher surfactant concentrations, such as System 2 (Exp. 6-8; 9-10 min) and System 3 (Exp. 13: 6.5 ± 0.1 min). PEG 400-based formulations consistently achieved faster self-emulsification than ethanol-based systems. Ethanol-containing formulations (Systems 3-4) displayed delayed emulsification, with most samples requiring more than 10 min to disperse completely. Among co-surfactant types, formulations incorporating Span 20, which has a higher HLB, generally emulsified more rapidly than those containing Span 80, a lower HLB surfactant. However, the relationship between self-emulsification time and droplet characteristics was not linear, as shorter emulsification times did not always correspond to smaller droplet size or low PDI. Overall, PEG 400-based systems containing Span 20 and adequate Cremophor RH40 demonstrated the most efficient self-emulsification behavior among the formulations evaluated.

3.3. Evaluation of selected SNEDDS formulations

Although the quadratic models developed for each SNEDDS system demonstrated high R^2 and adjusted R^2 values, the predicted R^2 values for most systems were found to be substantially low. These values indicate limited predictive capability, rendering the models unreliable for extrapolating beyond the experimental design space. Given this limitation, it was necessary to adopt an alternative, criteria-based strategy to identify promising formulations for further development. Therefore, at least one formulation from each SNEDDS system was selected based on its ability to incorporate a relatively high proportion of oil (castor oil), which is a key component in enhancing the solubility of lipophilic bioactive constituents of ginger extract.

To guide this selection, theoretical optimal compositions were generated using the point prediction

Table 5. Polydispersity index (PDI) values of droplets and self-emulsification time obtained after dispersing each SNEDDS system in 0.1 N hydrochloric acid

Exp No.	Composition (% w/w)				PDI values				Self-emulsification time (min)			
	Oil	Surfactant	Co-surfactant	Co-solvent	System 1	System 2	System 3	System 4	System 1	System 2	System 3	System 4
1	40.0	60.0	0.0	0.0	0.69 ± 0.02	0.37 ± 0.09	0.52 ± 0.02	0.48 ± 0.04	2.3 ± 0.4	5.1 ± 0.1	>10	>10
2	40.0	26.7	24.9	8.4	0.28 ± 0.02	0.12 ± 0.07	0.21 ± 0.10	0.17 ± 0.13	2.5 ± 0.8	1.4 ± 0.5	>10	>10
3	40.0	9.7	40.3	10.0	1.00 ± 0.00	0.84 ± 0.03	1.00 ± 0.00	0.58 ± 0.03	1.4 ± 0.1	>10	>10	>10
4	37.3	0.0	61.2	1.5	NA	0.54 ± 0.31	0.52 ± 0.12	0.70 ± 0.22	NA	>10	>10	>10
5	32.8	44.9	12.2	10.0	0.38 ± 0.09	0.14 ± 0.02	0.23 ± 0.03	0.27 ± 0.04	1.2 ± 0.9	>10	>10	>10
6	23.8	39.2	31.9	5.2	0.28 ± 0.10	0.15 ± 0.04	0.13 ± 0.01	0.15 ± 0.08	1.5 ± 1.0	9.0 ± 0.2	9.4 ± 0.7	>10
7	23.8	39.2	31.9	5.2	0.13 ± 0.10	0.17 ± 0.13	0.12 ± 0.11	0.14 ± 0.05	1.8 ± 0.8	10.1 ± 0.4	9.2 ± 0.1	>10
8	23.8	39.2	31.9	5.2	0.20 ± 0.02	0.15 ± 0.05	0.12 ± 0.04	0.16 ± 0.04	1.5 ± 0.5	10.0 ± 0.2	9.1 ± 0.3	>10
9	22.6	0.0	67.4	10.0	NA	0.41 ± 0.03	0.43 ± 0.03	0.46 ± 0.13	NA	>10	>10	>10
10	22.1	17.3	50.6	10.0	1.00 ± 0.00	0.29 ± 0.21	1.00 ± 0.00	0.46 ± 0.30	1.4 ± 0.8	>10	>10	>10
11	20.8	69.2	0.0	10.0	0.32 ± 0.15	0.27 ± 0.02	0.26 ± 0.08	0.40 ± 0.02	1.7 ± 0.2	10.3 ± 0.1	>10	>10
12	15.0	35.6	49.4	0.0	0.56 ± 0.04	0.42 ± 0.20	0.46 ± 0.21	0.26 ± 0.02	3.4 ± 0.4	>10	>10	>10
13	15.0	35.6	49.4	0.0	0.56 ± 0.02	0.49 ± 0.05	0.39 ± 0.13	0.43 ± 0.03	2.1 ± 0.2	>10	6.5 ± 0.1	>10
14	11.7	85.0	0.0	3.3	0.41 ± 0.04	0.28 ± 0.13	0.19 ± 0.09	0.23 ± 0.04	1.3 ± 0.6	10.2 ± 0.2	>10	>10
15	10.2	0.0	85.0	4.8	NA	0.49 ± 0.03	0.66 ± 0.21	0.57 ± 0.16	NA	>10	>10	>10
16	5.6	63.0	21.4	10.0	0.50 ± 0.06	0.46 ± 0.02	0.40 ± 0.03	0.41 ± 0.01	1.7 ± 0.4	10.1 ± 0.4	>10	>10
17	5.0	16.2	68.8	10.0	1.00 ± 0.00	0.26 ± 0.07	0.58 ± 0.02	0.46 ± 0.05	1.2 ± 0.9	>10	>10	NA
18	5.0	44.0	41.0	10.0	0.60 ± 0.05	0.27 ± 0.15	0.42 ± 0.02	0.19 ± 0.04	6.3 ± 0.3	>10	>10	NA

NA = Not completely dispersed within 20 min.

Table 6. Composition and characteristics of selected SNEDDS formulations (mean ± SD, *n* = 3)

System	SNEDDS formulations	Composition (% w/w)						Parameter			
		Oil	Surfactant	Co-surfactant		Co-solvent		Nanoemulsion Appearance	Self-emulsification time (min)	Particle size (nm)	PDI
		Castor oil	Cremophor RH 40	Span 80	Span 20	PEG 400	Ethanol				
1	F1	31.0	36.0	-	27.5	5.5	-	Transparent	3.3 ± 0.6	54.5 ± 0.1	0.17 ± 0.00
	F2	18.0	36.0	-	40.5	5.5	-	Translucent	NA	69.9 ± 1.7	0.52 ± 0.02
2	F3	39.5	38.0	17.0	-	5.5	-	Transparent	5.3 ± 0.4	64.1 ± 0.5	0.16 ± 0.01
	F4	18.0	36.0	40.5	-	5.5	-	Translucent	9.7 ± 0.3	71.8 ± 1.2	0.20 ± 0.00
3	F5	31.8	35.5	-	27.5	-	5.2	Transparent	4.3 ± 0.7	42.5 ± 0.5	0.12 ± 0.00
	F6	18.0	36.0	-	40.5	-	5.5	Translucent	15.3 ± 1.2	63.8 ± 1.4	0.58 ± 0.04
4	F7	20.0	74.0	0.5	-	-	5.5	Transparent	2.3 ± 0.6	33.9 ± 0.2	0.17 ± 0.01
	F8	18.0	36.0	40.5	-	-	5.5	Translucent	5.3 ± 1.4	78.1 ± 0.5	0.20 ± 0.00

NA = Not completely dispersed within 20 min.

and desirability function tools in Design-Expert® software. In the desirability function approach, all component constraints were maintained within the predefined design space, while particle size was set as the primary response to be minimize. Eight formulations of blank SNEDDS (F1-F8) with various concentrations and components were identified, as summarized in Table 6. All eight blank SNEDDS formulations met the predefined criteria for acceptable self-emulsifying nanoemulsion performance: (1) particle size ≤ 200 nm, (2) PDI ≤ 0.3, and (3) self-emulsification time ≤ 10 min. Among these, F1, F3, F4, F5, and F7 exhibited rapid emulsification (2–10 min), clear to slightly opalescent appearance, and droplet sizes below 72 nm, indicating efficient dispersion and adequate interfacial stabilization. In contrast, F2, F6, and F8, although still within the acceptable limits, showed relatively longer emulsification times or higher PDI values, likely due to lower surfactant content or higher co-surfactant proportions, which may weaken interfacial film strength. The smallest droplet size was observed in F7 (33.9 ± 0.2 nm), containing Span 80 and ethanol. The combination of a low-HLB co-surfactant (Span 80) with a volatile, low-viscosity co-solvent (ethanol) likely promoted efficient interfacial packing and rapid droplet dispersion. In comparison, PEG 400-based systems (F1–F4) demonstrated slightly larger droplet sizes, which can be attributed to the higher viscosity and hydrophilicity of PEG 400, which can slow droplet disruption and diffusion during emulsification. Overall, these results support the selection of F1, F3, F4, F5, and F7 as the most suitable blank SNEDDS formulations for subsequent drug-loading studies.

3.4. Evaluation of G-SNEDDS formulations

G-SNEDDS formulations were developed based on the optimized blank SNEDDS systems (Table 7). Incorporation of ginger extract did not markedly alter the emulsification behavior, indicating sufficient solubilization of the lipophilic constituents of the extract within the selected excipient matrices. All formulations produced clear to slightly translucent nanoemulsions with self-emulsification times ranging from 2.7 to 9.9 min, droplet sizes between 51.5 and 124.1 nm, and PDI values ≤ 0.35. Among the tested formulations, G-F1, G-F3, G-F4, G-F5, and G-F7 exhibited overall favorable physicochemical performance.

The smallest droplet size and fastest self-emulsification were observed for G-F7 (System 4: Span 80 with ethanol), with a self-emulsification time of 2.7 ± 0.8 min, a particle size of 51.5 ± 1.8 nm, and a PDI of 0.22 ± 0.01. PEG 400-based formulations, such as G-F1 and G-F5, showed slightly larger droplet sizes (62-72 nm) but maintained low PDI values (< 0.2) and good visual clarity. In contrast, formulations containing higher proportion of co-surfactant, such as G-F4, exhibited larger droplet sizes and moderately increased PDI values

Table 7. Composition and characteristics of G-SNEDDS formulations (mean ± SD, *n* = 3)

System	G-SNEDDS formulations	Composition (% w/w)							Parameter			
		Ginger extract	Oil	Surfactant	Co-surfactant		Co-solvent		Nanoemulsion Appearance	Self-emulsification time (min)	Particle size (nm)	PDI
			Castor oil	Cremophor RH 40	Span 80	Span 20	PEG 400	Ethanol				
1	G-F1	33.3	20.7	24.0	-	18.3	3.7	-	Transparent	9.3 ± 0.6	62.2 ± 0.8	0.10 ± 0.01
2	G-F3	33.3	26.3	25.3	11.3	-	3.7	-	Translucent	7.3 ± 0.5	70.0 ± 1.2	0.14 ± 0.01
	G-F4	33.3	12.0	24.0	27.0	-	3.7	-	Translucent	9.9 ± 0.6	87.6 ± 2.8	0.26 ± 0.01
5	G-F5	33.3	21.2	23.7	-	18.3	-	3.5	Transparent	6.3 ± 0.1	71.7 ± 0.2	0.15 ± 0.02
6	G-F7	33.3	13.3	49.3	0.3	-	-	3.7	Transparent	2.7 ± 0.8	51.5 ± 1.8	0.22 ± 0.01

(up to 0.26), suggesting reduced interfacial stabilization at elevated co-surfactant levels. Overall, all five selected formulations, G-F1, G-F3, G-F4, G-F5, and G-F7, fulfilled the physicochemical criteria for acceptable self-emulsifying nanoemulsions, with droplet sizes < 100 nm and emulsification times < 10 min.

3.5. EE of 6-gingerol and 6-shogaol in G-SNEDDS formulations

The EE of 6-gingerol and 6-shogaol in the G-SNEDDS formulations was determined by ultrafiltration followed by HPLC quantification (Table 8). All formulations exhibited high encapsulation efficiencies for both bioactive compounds, with EE values exceeding 90% in nearly all cases. For 6-gingerol, EE values ranged from 91.75 % (G-F5) to 96.33 % (G-F3), while for 6-shogaol, EE values ranged from 92.94 % (G-F7) to 95.54 % (G-F4). Formulations G-F3 and G-F4 exhibited the highest mean EE values for 6-gingerol and 6-shogaol, respectively. No statistically significant differences ($p > 0.05$) were observed among formulations for either compound, indicating comparable encapsulation efficiencies across the tested systems. These results demonstrate that all optimized G-SNEDDS formulations are suitable for efficiently encapsulating ginger-derived bioactive compounds, thereby providing a robust foundation for subsequent stability and *in vitro* release studies.

Table 8. Entrapment efficiency of 6-gingerol and 6-shogaol in various G-SNEDDS formulations (mean ± SD, *n* = 3)

G-SNEDDS Formulation	Entrapment efficiency (%)	
	6-Gingerol	6-Shogaol
G-F1	95.04 ± 4.06	94.74 ± 3.89
G-F3	96.33 ± 8.69	92.95 ± 2.79
G-F4	95.54 ± 5.11	95.54 ± 4.14
G-F5	91.75 ± 1.04	94.26 ± 3.22
G-F7	91.99 ± 0.26	92.94 ± 3.34

3.6. Morphological characterization of G-SNEDDS

TEM was employed to evaluate the morphological features and nanoscale structure of G-SNEDDS formulations. Figure 2 presents representative TEM micrographs of five selected formulations: G-F1, G-F3, G-F4, G-F5, and G-F7. The TEM images confirmed the formation of spherical and well-dispersed nanoemulsion droplets in formulations G-F1, G-F3, G-F4, and G-F5. These droplets exhibited relatively uniform morphology, smooth surfaces, and minimal aggregation, which are characteristic features of a physically stable

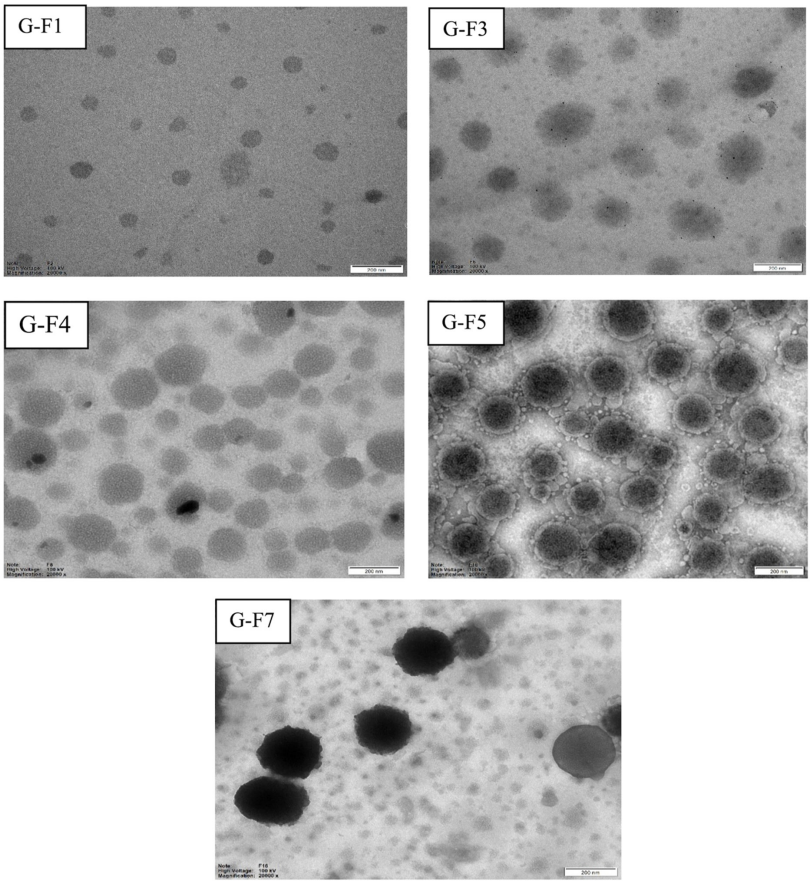

Figure 2. TEM images of G-SNEDDS formulations, including G-F1, G-F3, G-F4, G-F5, and G-F7. Scale bar: 200 nm.

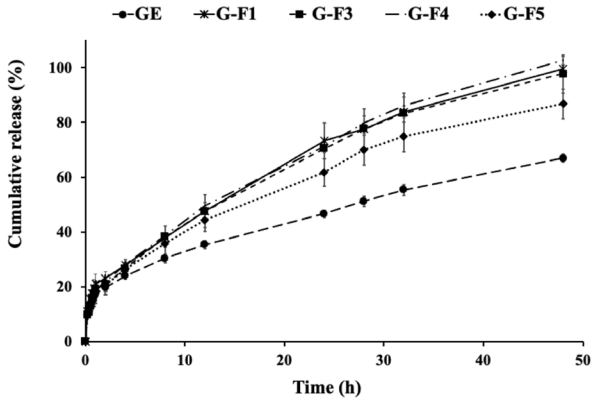

Figure 3. ***In vitro*** **cumulative release (%) of 6-gingerol from ginger extract (GE) and selected G-SNEDDS formulations (G-F1, G-F3, G-F4, and G-F5) over 48 h (mean ± SD, *n* = 3).**

nanoemulsion system. The observed nanoscale structures were generally consistent with the DLS results reported previously, in which these formulations demonstrated small droplet sizes (< 150 nm), low polydispersity indices (PDI < 0.3), and rapid self-emulsification behavior.

In contrast, G-F7 exhibited larger apparent particle sizes with evident aggregation in the TEM images, suggesting reduced interfacial stability of the emulsion system under the examined conditions. It is important to note that particle size values obtained by DLS, and morphological features observed by TEM do not necessarily correspond directly, as these techniques probe different physical states of the system. DLS measures the hydrodynamic diameter of droplets immediately after dispersion under high dilution conditions, whereas TEM visualizes droplets following sample preparation and drying, which may accentuate aggregation phenomena in formulations with limited interfacial stability, particularly those containing high proportions of volatile co-solvents such as ethanol.

Overall, the combined interpretation of TEM and DLS results provides a more comprehensive understanding of the physical behavior of the G-SNEDDS formulations, and further supports the suitability of G-F1, G-F3, G-F4, and G-F5 for continued development and drug delivery evaluation.

3.7. *In vitro* release study of G-SNEDDS

The *in vitro* release profiles of the pure ginger extract and selected G-SNEDDS formulations (G-F1, G-F3, G-F4, and G-F5) were investigated over a 48 h period in 0.1 N hydrochloric acid. As illustrated in Figure 3, all G-SNEDDS formulations exhibited significantly enhanced cumulative release of ginger extract compared to the unformulated control. After 48 h, the cumulative release of 6-gingerol from the G-SNEDDS formulations ranged from 88.54% to 102.52%, whereas the release from the pure ginger extract was markedly lower

Table 9. Physical stability studies of G-SNEDDS formulation

G-SNEDDS Formulation	Before heating-cooling cycle analysis				After heating-cooling cycle analysis			
	G-SNEDDS Appearance	Nanoemulsion Appearance	Particle Size (nm)	PDI	G-SNEDDS Appearance	Nanoemulsion Appearance	Particle Size (nm)	PDI
G-F1	Dark Brown, No phase separation	Transparent	61.5 ± 0.7	0.13 ± 0.01	Dark Brown, No phase separation	Transparent	61.5 ± 0.7	0.13 ± 0.01
G-F3	Dark Brown, No phase separation	Transparent	67.9 ± 0.5	0.09 ± 0.01	Dark Brown, No phase separation	Transparent and locculation	67.9 ± 0.5	0.09 ± 0.01
G-F4	Dark Brown, No phase separation	Transparent	87.1 ± 0.6	0.16 ± 0.02	Dark Brown, No phase separation	Translucent and locculation	87.1 ± 0.6	0.16 ± 0.02

*Significant difference compared to day 0 ($p < 0.05$).

Table 10. Droplet size of G-SNEDDS formulations (G-F1, G-F3, and G-F4) over a 90-day short-term storage period at 4°C, 30°C, and 45°C (mean ± SD, *n* = 3)

G-SNEDDS Formulation	Day 0	Day 30			Day 60			Day 90		
		4°C	30°C	45°C	4°C	30°C	45°C	4°C	30°C	45°C
G-F1	59.8 ± 1.6	60.2 ± 2.2	62.1 ± 1.7	64.2 ± 1.9	59.2 ± 2.0	63.9 ± 2.1	67.7 ± 2.0*	60.2 ± 2.2	65.3 ±1.7	72.2 ± 1.2*
G-F3	69.9 ± 2.2	70.5 ± 1.9	72.5 ± 2.2	73.2 ± 1.8	69.9 ± 1.9	73.5 ± 2.2	77.1 ± 1.1*	69.7 ± 1.4	76.3 ± 1.7*	81.8 ± 2.3*
G-F4	89.8 ± 1.6	90.0 ± 1.5	92.0 ± 1.3	94.5 ± 1.5*	89.9 ± 2.7	93.8 ± 1.8*	97.9 ± 2.1*	91.0 ± 1.2	95.7 ± 1.5*	102.4 ± 1.7*

*Significant difference compared to day 0 ($p < 0.05$).

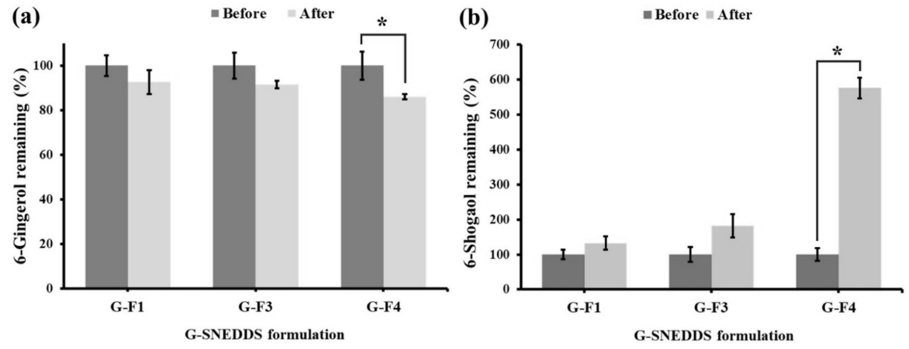

Figure 4. The percentage of 6-gingerol (a) and 6-shogaol (b) remaining in G-SNEDDS formulations (G-F1, G-F3, and G-F4) before and after the heating-cooling cycle. An asterisk (*) indicates a statistically significant difference compared to the values before the heating-cooling cycle ($p < 0.05$).

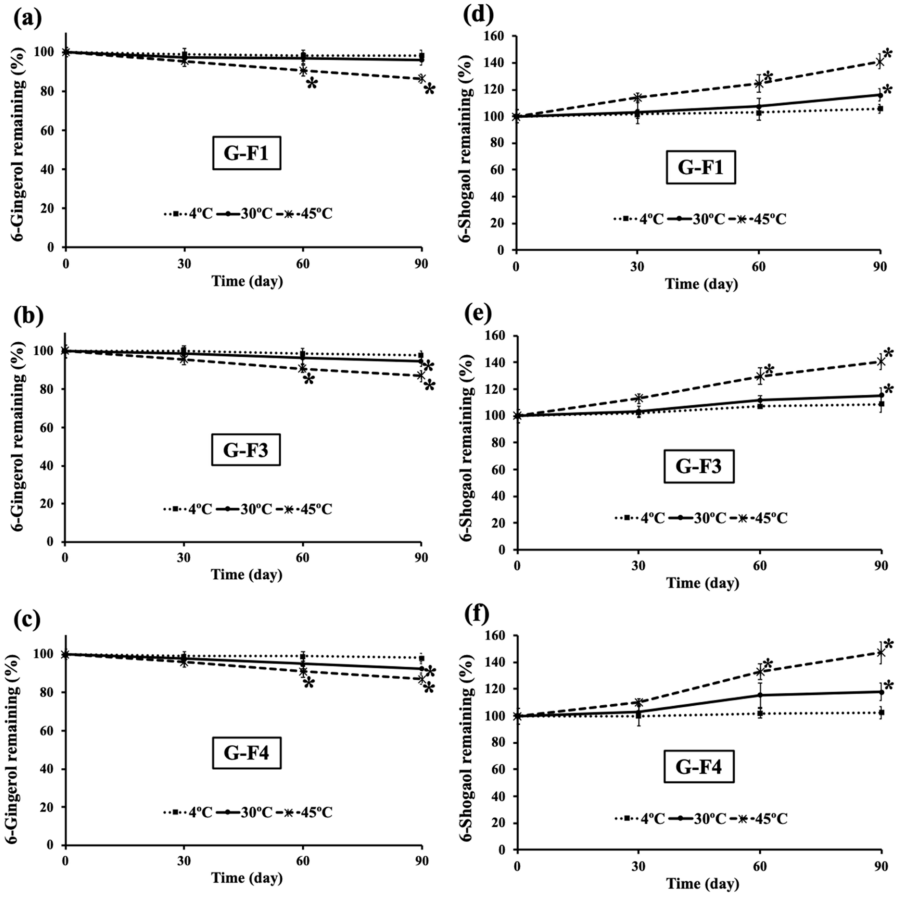

Figure 5. Stability profiles of 6-gingerol (a-c) and 6-shogaol (d-f) remaining (%) in G-SNEDDS formulations: G-F1, G-F3, and G-F4, stored at 4 °C, 30°C, and 45°C over 90 days. Data are presented as mean ± SD ($n = 3$). Asterisks (*) indicate statistically significant differences compared to Day 0 ($p < 0.05$).

at 66.95%. Among the formulations tested, G-F4 demonstrated the highest cumulative drug release (102.52%), followed by G-F1, G-F3, and G-F5. The enhanced release profile can be attributed to the spontaneous formation of fine nanoemulsions upon dilution, with droplet sizes < 200 nm, as previously confirmed by DLS and TEM analyses.

3.8. Stability study of G-SNEDDS

3.8.1. Heating-cooling cycle analysis

The physical stability of selected G-SNEDDS formulations (G-F1, G-F3, and G-F4) was evaluated under thermal stress using a heating-cooling cycle analysis. The results are presented in Table 9. All formulations initially presented as transparent nanoemulsions with dark brown coloration, with no visible phase separation, indicating successful self-

emulsification and homogeneity. After completion of the heating-cooling cycles, G-F1 retained its original appearance and demonstrated the most robust physical stability, with no statistically significant changes in particle size and PDI.

In contrast, G-F3 exhibited a slight increase in particle size (from 67.9 ± 0.5 nm to 70.5 ± 1.2 nm) and a minor increase in PDI (0.09 ± 0.01 to 0.10 ± 0.01), accompanied by the onset of flocculation, indicating moderate physical instability. The most physical instability was observed for G-F4, which showed marked increases in particle size (67.1 ± 0.6 nm to 97.7 ± 1.1 nm) and PDI (0.16 ± 0.02 to 0.33 ± 0.01), with clear flocculation and a visible change in appearance from transparent to translucent.

The chemical stability of G-F1, G-F3, and G-F4 under heating-cooling conditions was evaluated by quantifying the concentration of 6-gingerol and 6-shogaol before and after themal stress, as shown in Figure 4. Following thermal cycling, all formulations exhibited a reduction in 6-gingerol content, indicating thermal degradation of this compound. Conversely, the concentration of 6-shogaol increased significantly, particularly in G-F4. G-F4 exhibited the highest increase in 6-shogaol content, reaching 576.1 ± 28.9 % after heating-cooling treatment, corresponding to a > 4-fold increase ($p < 0.001$). In contrast, G-F1 and G-F3 showed only modest increases in 6-shogaol levels and smaller reductions in 6-gingerol content, indicating greater chemical stability compared with G-F4.

3.8.2. Short-term storage stability study

The stability of the G-SNEDDS formulations during short-term storage was assessed by monitoring changes in droplet size and the remaining percentages of 6-gingerol and 6-shogaol over 90-day period under different temperature conditions. The results presented in Table 10 demonstrate a significant temperature-dependent increase in droplet size for all formulations. At day 0, the initial droplet sizes for G-F1, G-F3, and G-F4 were 59.8 ± 1.6 nm, 69.9 ± 2.2 nm, and 89.8 ± 1.6 nm, respectively. Throughout the 90-day storage period, G-F1 remained relatively stable at 4°C and 30°C, with not statistically significant change observed ($p > 0.05$). However, at 45°C, G-F1 showed a significant increase in droplet size, reaching 72.2 ± 1.2 nm on day 90 ($p < 0.05$). Similarly, G-F3 and G-F4 exhibited significant increases in droplet size at 45°C, reaching 81.8 ± 2.3 nm and 102.4 ± 1.7 nm, respectively, indicating thermal-induced instability of the nanoemulsion droplets. Among the three formulations, G-F1 exhibited the highest overall physical stability in terms of maintaining its droplet size across all tested storage temperatures.

Figure 5 illustrates the degradation and transformation profiles of 6-gingerol and 6-shogaol during the storage period. A gradual decline in 6-gingerol content was observed in all formulations, particularly under elevated temperature conditions. At 45°C, 6-gingerol degradation was significantly accelerated, with remaining contents dropping to 86.5%, 81.8%, and 86.9% in G-F1, G-F3, and G-F4, respectively, on day 90 ($p < 0.05$). The reduction in 6-gingerol content is consistent with its known sensitivity to heat, light, and oxygen, leading to thermal degradation and dehydration reactions. In contrast, the content of 6-shogaol increased progressively with both storage time and temperature, suggesting an interconversion process in which 6-gingerol underwent dehydration to form 6-shogaol. This transformation was most pronounced in G-F4, which exhibited the highest remaining percentage of 6-shogaol (140.6%) at 45°C on day 90. G-F1 and G-F3 also showed elevated 6-shogaol levels at higher temperatures, although to a lesser extent. The consistent increase in 6-shogaol content at 45°C further supports the occurrence of the thermally induced conversion of 6-gingerol into its dehydrated analog during storage.

4. Discussion

The extraction time significantly affected both the extraction yield and phytochemical composition of the ginger extracts. As expected, prolonging the extraction time to 30 min increased the crude yield, likely due to enhanced solvent penetration and more extensive cell wall disruption, which facilitated solute diffusion (*19*). However, the 10-min extract exhibited the highest 6-gingerol content, suggesting that extended extraction durations may induce degradation of thermolabile constituents (*20*).

This observation aligns with previous reports indicating that 6-gingerol is sensitive to heat and prolonged extraction, undergoing dehydration and oxidation to 6-shogaol and other degradation products, particularly under elevated temperature or acidic conditions (*21*). The reduced 6-gingerol content observed in the 20- and 30-min extracts supports this degradation trend. In contrast, 6-shogaol levels remained relatively constant across the different extraction times, implying that the mild temperature employed in this study was insufficient to promote time-dependent conversion of 6-gingerol into 6-shogaol (*22*). Therefore, considering the balance between extraction yield and bioactive stability, a 10-min extraction time appears optimal for maximizing 6-gingerol retention.

Further investigation into the formulation phase revealed that the type and concentration of excipients critically governed droplet formation, size distribution, and emulsification efficiency in the SNEDDS. The co-solvent markedly influenced on system behavior, PEG 400 increased droplet size and heterogeneity, which can be attributed to its high viscosity and hydrogen-bonding potential that hinder interfacial mobility (*23*). In contrast, ethanol promoted the formation of smaller droplets and

faster emulsification by facilitating interfacial disruption and rapid solvent exchange. Nevertheless, excessive ethanol in combination with insufficient surfactant levels destabilized the interfacial film, resulting in broader size distributions (*24*).

The surfactant–co-surfactant ratio was also a critical determinant of nanoemulsion performance. Formulations containing sufficient Cremophor RH40 (≥ 35% w/w) and moderate co-surfactant levels (20-35% w/w) yielded small droplets with narrow PDI values, reflecting effective interfacial stabilization. Conversely, low surfactant concentrations or excessive co-surfactant content disrupted interfacial cohesion, resulting in multimodal droplet size distributions (*25*).

The type of co-surfactant also influenced self-emulsification behavior. Span 80, a low HLB surfactant, exhibited stronger affinity for the oil phase and promoted tighter interfacial packing than Span 20, thereby enhancing interfacial elasticity when combined with the high-HLB surfactant, Cremophor RH40 (*26*). In ethanol-based systems, this combination facilitated the formation of smaller and more uniform droplets. However, despite the favorable initial droplet size observed in systems containing Span 80 and ethanol (such as G-F7), these formulations exhibited physical instability over time, as evidenced by pronounced droplet aggregation. This phenomenon may be attributed to the high volatility of ethanol, which can rapidly diffuses into the continuous aqueous phase upon dilution, thereby reducing the effective surfactant concentration available to maintain the integrity of the interfacial film (*27*). Furthermore, although Span 80 enhances interfacial elasticity, its combination with high concentration of volatile co-solvents can lead to a transiently stable film that is susceptible to thinning and subsequent droplet coalescence during long-term storage or under environmental stress. In contrast, Span 20 promoted rapid but comparatively less stable emulsification, consistent with its higher hydrophilicity.

Overall, solvent polarity and surfactant composition jointly governed emulsification efficiency. PEG 400-based systems exhibited slower dispersion due to reduced interfacial mobility, whereas ethanol-based systems required higher surfactant levels to counteract transient interfacial destabilization during dilution (*28*). Among all tested systems, those incorporating Span 80 and Cremophor RH40 demonstrated the most favorable balance between interfacial flexibility and stability, consistent with previously reported findings (*29*). Incorporation of ginger extract did not adversely affect emulsification behavior, confirming its compatibility with the selected lipid excipients. Consequently, ethanol-based SNEDDS containing Span 80 and Cremophor RH40 achieved rapid self-emulsification, small droplet size, and narrow size distributions, features that collectively enhance solubility and the potential oral bioavailability of the ginger extract.

The consistently high entrapment efficiencies (> 90%) observed across all G-SNEDDS formulations confirm the strong lipophilic affinity of 6-gingerol and 6-shogaol. Their hydrophobic nature favors preferential partitioning into the oil and surfactant domains, resulting in efficient encapsulation within the lipid matrix rather than the aqueous phase. Comparable high loading efficiencies of 6-gingerol have been reported in solid lipid nanoparticles and liposomal systems, which further support the present findings (*30,31*).

The enhanced drug release profile of G-SNEDDS can be attributed to the spontaneous formation of fine oil-in-water nanoemulsions upon dilution, which substantially increases the interfacial surface area and facilitates rapid drug solubilization and diffusion (*32*). In addition, amphiphilic surfactants and co-surfactants enhance interfacial fluidity, thereby accelerating drug partitioning and diffusion across the oil-water interface. These mechanisms are consistent with the improved dissolution and absorption commonly reported for SNEDDS-based delivery systems (*23*).

The degradation pattern of 6-gingerol under thermal and storage stress further highlights the importance of formulation design and appropriate storage control. The transformation of 6-gingerol to 6-shogaol *via* intramolecular dehydration is well documented under thermal and oxidative conditions (*4,5*). Accordingly, the elevated levels of 6-shogaol observed in formulation G-F4 are indicative of thermally induced conversion of 6-gingerol, consistent with its established dehydration pathway under heat and oxidative stress. Among all systems evaluated, G-F1 exhibited the highest physicochemical and chemical stability, maintaining consistent droplet size, low PDI values, and minimal degradation during both accelerated and long-term storage. This enhanced stability can be attributed to an optimized surfactant-to-co-surfactant ratio, which promotes the formation of a cohesive interfacial film, thereby minimizing droplet coalescence and restricting molecular mobility under thermal stress.

Temperature exerted a strong influence on formulation stability: all formulations remained physically stable at 4°C and 30°C, whereas exposure to 45°C significantly accelerated the degradation of 6-gingerol and the formation of 6-shogaol. These results corroborate previous studies demonstrating that high-temperature storage of ginger oleoresin promotes dehydration of 6-gingerol (*33,34*). Collectively, the findings indicate that SNEDDS can effectively preserve 6-gingerol under short-term storage conditions by maintaining a stabilized lipidic microenvironment, although complete protection against heat-induced conversion cannot be achieved. Despite these advantages, the present study has certain limitations. The physicochemical performance of SNEDDS following dilution and exposure to simulated gastrointestinal conditions was not evaluated. *In vivo*, SNEDDS are

subjected to dynamic physiological processes, including dilution, enzymatic digestion, and bile salt interaction, which can markedly influence droplet integrity and drug solubilization (*35*). Therefore, future studies should investigate the stability and performance of the optimized formulations under simulated gastrointestinal digestion conditions to better predict their *in vivo* behavior. Among the formulations evaluated, G-F1 exhibited the most robust physicochemical integrity and chemical stability, thereby identifying it as the most promising candidate for long-term storage and further development.

5. Conclusions

In this study, a G-SNEDDS was successfully developed to overcome the poor water solubility and instability of ginger's bioactive constituents. UAE for 10 min was identified as the optimal extraction condition for maximizing 6-gingerol content while maintaining an acceptable extract yield. Using a DoE-guided optimization approach, an optimized SNEDDS formulation, comprising castor oil as the lipid phase, Cremophor RH40 as the surfactant, Span 20 or Span 80 as the co-surfactant, and a low proportion of PEG 400 as the co-solvent, achieved rapid self-emulsification, producing fine nanoemulsion droplets with a uniform size distribution. This formulation encapsulated more than 90% of the ginger bioactives and demonstrated compliance with essential performance criteria, including droplet size, PDI, and emulsification efficiency.

The optimized G-SNEDDS significantly enhanced the dissolution profile of 6-gingerol compared to the unformulated extract, indicating a strong potential for enhanced oral bioavailability. In addition, the system demonstrated good physical stability under ambient and refrigerated storage conditions, with minimal changes in particle size over a three-month period. A slight degradation of 6-gingerol to 6-shogaol was observed under accelerated high-temperature conditions, highlighting the importance of appropriate storage conditions. Overall, this work demonstrates that incorporation of ginger extract into a lipid-based nanoemulsion system is an effective strategy to enhance solubility and protect thermosensitive constituents. The SNEDDS approach developed herein shows considerable promise for improving the therapeutic efficacy of ginger and other poorly water-soluble phytochemicals, thereby supporting further *in vivo* evaluation for oral supplementation and drug delivery applications.

Acknowledgements

The authors are grateful to the Faculty of Pharmacy, Chiang Mai University for their support. The authors would like to thank and gratefully acknowledge Kanyanut Suksumran, Vasinpong Prembanyat, Praewa Makmee, Chayaporn Fongkham, and Goekpon Yoocharoen for their assistance in conducting the experiments for this research project.

Funding: This work was supported by a grant from CMU Junior Research Fellowship program, Chiang Mai University (Grant number: JRCMU2566R_014). Maung Maung Than expresses sincere gratitude for the Teaching Assistant and Research Assistant (TA/RA) scholarship provided by Chiang Mai University.

Conflict of Interest: The authors have no conflicts of interest to disclose.

References

1. Mashhadi NS, Ghiasvand R, Askari G, Hariri M, Darvishi L, Mofid MR. Anti-oxidative and anti-inflammatory effects of ginger in health and physical activity: Review of current evidence. Int J Prev Med. 2013; 4:36-42.
2. Ali BH, Blunden G, Tanira MO, Nemmar A. Some phytochemical, pharmacological and toxicological properties of ginger (*Zingiber Officinale Roscoe*): A review of recent research. Food Chem Toxicol. 2008; 46:409-420.
3. Ghasemzadeh A, Jaafar HZE, Rahmat A. Antioxidant activities, total phenolics and flavonoids content in two varieties of Malaysia young ginger (*Zingiber Officinale Roscoe*). Molecules. 2010; 15:4324-4333.
4. Semwal RB, Semwal DK, Combrinck S, Viljoen AM. Gingerols and shogaols: Important nutraceutical principles from ginger. Phytochemistry. 2015; 117:554-568.
5. Bhattarai S, Tran VH, Duke CC. The stability of gingerol and shogaol in aqueous solutions. J Pharm Sci. 2001; 90:1658-1664.
6. Pan MH, Hsieh MC, Kuo JM, Lai CS, Wu H, Sang S, Ho CT. 6-shogaol induces apoptosis in human colorectal carcinoma cells *via* ROS production, caspase activation, and GADD 153 expression. Mol Nutr Food Res. 2008; 52:527-537.
7. Ekor M. The growing use of herbal medicines: Issues relating to adverse reactions and challenges in monitoring safety. Front Pharmacol. 2014; 4:1-10.
8. Wei Q, Yang Q, Wang Q, Sun C, Zhu Y, Niu Y, Yu J, Xu X. Formulation, characterization, and pharmacokinetic studies of 6-gingerol-loaded nanostructured lipid carriers. AAPS Pharm Sci Tech. 2018; 19:3661-3669.
9. Abdelaziz MA, Alalawy AI, Sobhi M, Alatawi OM, Alaysuy O. Development and characterization of engineered gingerol loaded chitosan nanoparticles for targeting colon cancer, bacterial infection, and oxidative stress mitigation. Int J Biol Macromol. 2025; 321(Pt1):146093.
10. Akram A, Rasul A, Waqas MK, Irfan M, Khalid SH, Aamir MN, Murtaza G, Ur Rehman K, Iqbal M, Khan BA. Development, characterization and evaluation of *in-vitro* anti-inflammatory activity of ginger extract based micro emulsion. Pak J Pharm Sci. 2019; 32:1327-1332.
11. Xu Y, Wang Q, Feng Y, Firempong CK, Zhu Y, Omari-Siaw E, Zheng Y, Pu Z, Xu X, Yu J. Enhanced oral bioavailability of [6]-gingerol-smedds: Preparation, *in vitro* and *in vivo* evaluation. J Funct Foods. 2016; 27:703-710.
12. Wijayanti II, Budiharjo A, Pangastuti A, Prihapsara F, Artanti AN. Total phenolic content and antioxidant

activity of ginger extract and SNEDDS with eel fish bone oil (*Anguilla spp.*). Nusantara Biosci. 2018; 10:164-169.
13. Singh B, Bhatowa R, Tripathi C, Kapil R. Developing micro-/nanoparticulate drug delivery systems using "design of experiments." Int J Pharm Investig. 2011; 1:75-87.
14. Kheawfu K, Pikulkaew S, Rades T, Müllertz A, von Gersdorff Jørgensen L, Okonogi S. Design and optimization of self-nanoemulsifying drug delivery systems of clove oil for efficacy enhancement in fish anesthesia. J Drug Deliv Sci Technol. 2021; 61:102241.
15. Gonzalez-Gonzalez M, Yerena-Prieto BJ, Carrera C, Vázquez-Espinosa M, González-de-Peredo AV, García-Alvarado MÁ, Palma M, Rodríguez-Jimenes G del C, Barbero GF. Optimization of an ultrasound-assisted extraction method for the extraction of gingerols and shogaols from ginger (*Zingiber Officinale*). Agronomy. 2023; 13:2-16.
16. Thai Pharmacopoeia Committee Thai Herbal Pharmacopoeia 2021: Bureau of drug and narcotic, department of medical sciences, ministry of public health. Available online: *https://bdn.go.th/thp/home*. (accessed on 1 August 2025).
17. Bu H, He X, Zhang Z, Yin Q, Yu H, Li Y. A TPGS-incorporating nanoemulsion of paclitaxel circumvents drug resistance in breast cancer. Int J Pharm. 2014; 471:206-13.
18. Kheawfu K, Panraksa P, Jantrawut P. Formulation and characterization of nicotine microemulsion-loaded fast-dissolving films for smoking cessation. Molecules. 2022; 27:3166.
19. Azwanida NN. A review on the extraction methods use in medicinal plants, principle, strength and limitation. Med Aromat Plants. 2015; 4:1-6.
20. Zagórska J, Czernicka-Boś L, Kukula-Koch W, Szalak R, Koch W. Impact of thermal processing on the composition of secondary metabolites of ginger rhizome: A review. Foods. 2022; 11:1-23.
21. Jiang H, Sólyom AM, Timmermann BN, Gang DR. Characterization of gingerol-related compounds in ginger rhizome (*Zingiber Officinale Rosc*.) by high-performance liquid chromatography/electrospray ionization mass spectrometry. Rapid Commun Mass Spectrom. 2005; 19:2957-2964.
22. Jung MY, Lee MK, Park HJ, Oh EB, Shin JY, Park JS, Jung SY, Oh JH, Choi DS. Heat-induced conversion of gingerols to shogaols in ginger as affected by heat type (dry or moist heat), sample type (fresh or dried), temperature and time. Food Sci Biotechnol. 2017; 27:687-693.
23. Buya AB, Beloqui A, Memvanga PB, Préat V. Self-nanoemulsifying drug delivery systems: From the development to the current applications and challenges in oral drug delivery. Pharmaceutics. 2020; 12:1-55.
24. Porter CJH, Trevaskis NL, Charman WN. Lipids and lipid-based formulations: Optimizing the oral delivery of lipophilic drugs. Nat Rev Drug Discov. 2007; 6:231-248.
25. Lawrence MJ, Rees GD. Microemulsion-based media as novel drug delivery systems. Adv Drug Deliv Rev. 2000; 45:89-121.
26. Pouton CW, Porter CJH. Formulation of lipid-based delivery systems for oral administration: Materials, methods and strategies. Adv Drug Deliv Rev. 2008; 60:625-637.
27. Guzey D, McClements DJ. Formation, stability and properties of multilayer emulsions for application in the food industry. Adv Colloid Interface Sci. 2006; 128-130:227-248.
28. Chen YS, Chiu YH, Li YS, Lin EY, Hsieh DK, Lee CH, Huang MH, Chuang HM, Lin SZ, Harn HJ, Chiou TW. Integration of PEG 400 into a self-nanoemulsifying drug delivery system improves drug loading capacity and nasal mucosa permeability and prolongs the survival of rats with malignant brain tumors. Int J Nanomedicine. 2019; 14:3601-3613.
29. Zeng L, Xin X, Zhang Y. Development and characterization of promising cremophor EL-stabilized o/w nanoemulsions containing short-chain alcohols as a cosurfactant. RSC Adv. 2017; 7:19815-19827.
30. Bhalekar MR, Madgulkar A, Jagtap TV. Demonstration of lymphatic uptake of (6)-gingerol solid lipid nanoparticles. J Drug Del Ther. 2019; 9:461-469.
31. Thangavelu P, Sundaram V, Gunasekaran K, Mujyambere B, Raju S, Kannan A, Arasu A, Krishna K, Ramamoorthi J, Ramasamy S, Velusamy T, Samiappan S. Development of optimized novel liposome loaded with 6-gingerol and assessment of its therapeutic activity against NSCLC *in vitro* and *in vivo* experimental models. Chem Phys Lipids. 2022; 245:105206.
32. Salawi A. Self-emulsifying drug delivery systems: A novel approach to deliver drugs. Drug Deliv. 2022; 29:1811-1823.
33. Oriani VB, Alvim ID, Paulino BN, Procópio FR, Pastore GM, Hubinger MD. The influence of the storage temperature on the stability of lipid microparticles containing ginger oleoresin. Food Res Int. 2018; 109:472-480.
34. Bhattarai S, Tran VH, Duke CC. Stability of [6]-gingerol and [6]-shogaol in simulated gastric and intestinal fluids. J Pharm Biomed Anal. 2007; 45:648-653.
35. Buya AB, Beloqui A, Memvanga PB, Préat V. Self-nano-emulsifying drug-delivery systems: From the development to the current applications and challenges in oral drug delivery. Pharmaceutics. 2020; 12:1194.

Received November 14, 2025; Revised February 4, 2026; Accepted February 6, 2026.

**Address correspondence to:*
Kantaporn Kheawfu, Department of Pharmaceutical Sciences, Faculty of Pharmacy, Chiang Mai University, Chiang Mai, 50200, Thailand.
E-mail: kantaporn.kheawfu@cmu.ac.th

Released online in J-STAGE as advance publication February 13, 2026.